Available online at www.sciencedirect.com

ScienceDirect

Mendeleev Commun., 2024, **34**, 595–597

Mendeleev Communications

Photoluminescence and thermoluminescence studies of Dy^{3+}-activated $LaCePO_4$ phosphor

K. Lakshmi,[a] M. C. Rao,*[a,b] Vikas Dubey[c] and K. V. R. Murthy[d]

[a] *Department of Physics, Krishna University, 521004 Machilipatnam, India*
[b] *Department of Physics, Andhra Loyola College, 520008 Vijayawada, India. E-mail: raomc72@gmail.com*
[c] *Department of Physics, North-Eastern Hill University, Shillong, 793022 Meghalaya, India. E-mail: jsvikasdubey@gmail.com*
[d] *Department of Applied Physics, Faculty of Engineering and Technology, M. S. University of Baroda, 390001 Vadodara, India*

DOI: 10.1016/j.mencom.2024.06.041

The $LaCePO_4$:Dy^{3+} luminescence experiments revealed the excitation peak at 275 nm which gives the emission spectra in visible region with intensive peaks centered at 475 and 573 nm. The emission spectra showed the transition from $^4F_{9/2}$ to the ground energy state. The prepared phosphor may be useful for display applications in white light emission and thermoluminescence dosimeters.

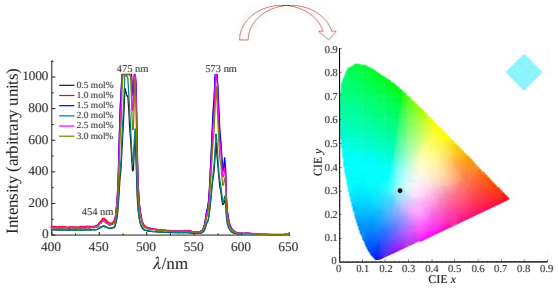

Keywords: $LaCePO_4$:Dy^{3+} phosphors, solid state lighting, XRD, SEM, CIE, white light emission.

White light emitting diodes (WLEDs) have a lot of advantages over the existing incandescent and halogen lamps in terms of power, efficiency, reliability, and long lifetime.[1,2] The remarkable progress has been made in the development of WLEDs using InGaN chips whose emission bands shift to the near-ultraviolet (near-UV) range around 400 nm.[3,4] Since UV-LEDs can offer highly efficient solid state light, more attention has been paid to the development of new phosphors that can be excited in the range of near-UV (350–420 nm) due to the necessity to increase the efficiency of white light emitting solid-state devices.[5] Alkaline earth silicates $R_2MgSi_2O_7$ (R = Ca, Sr, and Ba) co-doped with Eu^{2+} and Dy^{3+} having akermanite-based structures attract great attention in the development of persistent lighting.[6] The $CaMgSi_2O_6$, and $CaMgSi_2O_7$ phosphors activated with Eu^{2+}, Dy^{3+} and Nd^{3+} with afterglow characteristics were prepared by Jiang *et al.*[7] through solid-state reaction in a reducing atmosphere. Long-persistence phosphorescence in Ce^{3+}-doped $Ca_2Al_2SiO_7$ with a melilite structure has been reported by Kodama *et al.*[8,9] Phosphors like $BaMg_2Si_2O_7$ doped with Eu^{2+}- and Mn^{2+}, $CdSiO_3$:Mn^{2+}:RE (RE = Y, La, Gd, and Lu), Eu and Dy-doped $R_3MgSi_2O_8$ (R = Ca, Sr, and Ba), blue-emitting Eu^{2+}- and Dy^{3+}-doped $Sr_2ZnSi_2O_7$, and $CaAl_2Si_2O_8$ doped with Eu^{2+} and Dy^{3+} are reported as efficient long-lasting phosphors.[10–14]

In this work the spectroscopic parameters of Dy^{3+}-activated $LaCePO_4$ phosphor and the formation of nanoparticles of the synthesized phosphor are reported for the first time. The phosphor was synthesized by the modified solid-state reaction method and phase composition and morphology of the samples were determined by X-ray diffraction (XRD) and scanning electron microscopy (SEM). Photoluminescence (PL) analysis of the prepared phosphors was performed at various doping ion concentrations.

The $LaCePO_4$:Dy^{3+} phosphors were prepared by solid-state reaction technique with varying concentration of Dy^{3+} ions (0.5 to 3.0 mol%). La_2O_3, CeO_2, $NH_4H_2PO_4$, and Dy_2O_3 were used as starting materials at a proper stoichiometric ratio; H_3BO_3 (1.6 mol%) was used as a flux. All materials were thoroughly ground for ~ 2 h (using acetone for liquid grinding) to obtain a homogeneous powder using mortar and pestle. The ground mixture was transferred to the alumina crucible and heated at 800 °C for 2 h in a muffle furnace. The calcined sample was ground again and heated at 1150 °C for 4 h. The final calcined samples were ground to form fine powder and used for further characterization.

XRD diffractograms were recorded using a Bruker AXS D8 Advance X-ray Powder Diffractometer with Cu-Kα radiation (1.5406 Å) in 2θ range of 4–80°. SEM images were recorded using a JEOL JSM-6390LV scanning electron microscope, and PL excitation and emission spectra were monitored using a Shimadzu spectrophotofluorimeter. The Commission internationale de l'éclairage (CIE) chromaticity coordinates were calculated from the emission spectra of the phosphor samples using LUMPAC software. Thermoluminescence (TL) glow curves were recorded using a TLD I1009 reader supplied by Nucleonix Systems Pvt. Ltd.

The XRD patterns of the prepared pure and 2.5 mol% Dy^{3+}-doped $LaCePO_4$ phosphors and the phase composition are shown in Figure 1. The crystallite size of the sample was calculated from the full width at half maximum (FWHM) of all peaks in the XRD pattern using the Scherrer formula.[15–24] The crystallite size for the intense peak in the XRD pattern of the prepared $LaCePO_4$:Dy^{3+} (2.5 mol%) phosphor was found to be 41.81 nm.

Figures 2(*a*)–(*d*) show the SEM images of the Dy^{3+} (2.5 mol%)-activated $LaCePO_4$ phosphor at different magnifications. The prepared phosphor has a cube-like structure clearly visible in the 1 μm to 100 nm size range. This nanocube type of the

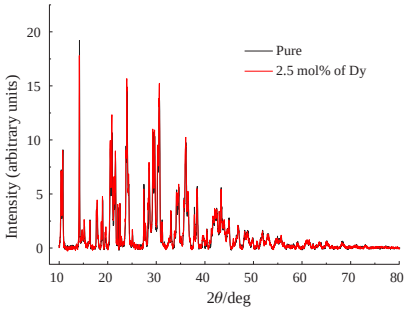

Figure 1 XRD patterns of pure and Dy^{3+} (2.5 mol%)-activated $LaCePO_4$ phosphors.

structure minimizes light scattering on the crystallite surface and enhances luminescence efficiency of the prepared phosphor. It is confirmed that the particles are uniformly distributed and should be useful for different practical applications in optoelectronics.

The PL excitation spectrum is recorded for the $LaCePO_4$ phosphor doped with 2.5 mol% of Dy^{3+} [Figure 3 (*a*)]. The broad emission peak centered at 275 nm is due to the charge transfer phenomenon of the O^{2-}–Dy^{3+} ion. The emission spectra were monitored at 275 nm excitation and several distinct peaks in the visible region centered at 475 nm (blue emission) and 573 nm (yellow one) having excellent PL emission intensity were revealed [Figure 3(*b*)]. The emission spectra show interesting features of the Dy^{3+} ion in the host lattice displaying blue and yellow emission simultaneously. The emission originates from the transition from the $^4F_{9/2}$ level to the ground state and other excited energy levels of the Dy^{3+} ion. Overall composed peaks resulted in white light emission confirmed by CIE coordinates.

The CIE chromaticity coordinates of the $LaCePO_4$:Dy^{3+} (2.5 mol%) phosphor shown in Figure 3(*c*) are calculated from the corresponding emission spectrum. The CIE coordinates of the phosphor are expressed in (*x*, *y*) and the values are found in the deep bluish-white region (touching the white light boundary). This clearly shows that the Dy^{3+}-doped $LaCePO_4$ sample can be used for white light emitting applications such as solid-state lighting and display device applications and its chromaticity coordinates are $x = 0.26$ and $y = 0.30$.[25]

Figure 4(*a*) shows the TL glow curves of the $LaCePO_4$ phosphor doped with Dy^{3+} (2.5 mol%) after UV exposure for various time. The TL glow curve intensity increases with increasing UV exposure time and the linear response to dose is found (see Online Supplementary Materials). Herein, the broad peak centered at 178ºC shows the composite nature, its deconvolution shows five distinct peaks, and the corresponding trap parameters are calculated using computerized glow curve deconvolution (CGCD) technique.[26–28] The trap parameters such as trap depth (activation energy), order of kinetics using shape

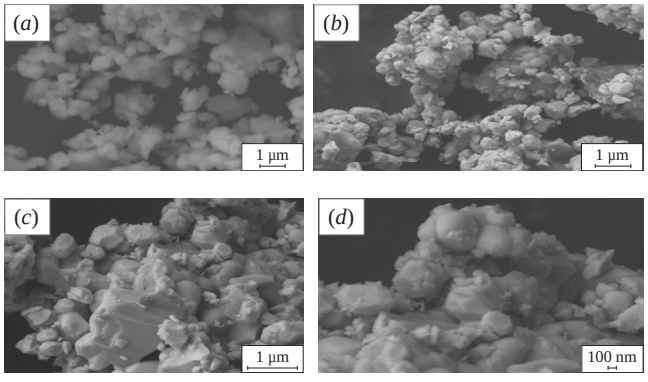

Figure 2 SEM images of Dy^{3+} (2.5 mol%)-activated $LaCePO_4$ phosphor at various magnifications.

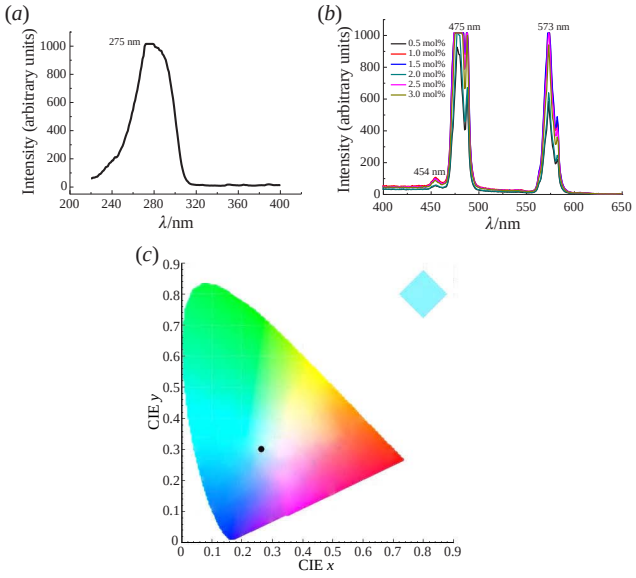

Figure 3 (*a*) PL excitation spectrum of $LaCePO_4$:Dy^{3+} (2.5 mol%) phosphors, (*b*) PL emission spectra of $LaCePO_4$:Dy^{3+} (0.5–3.0 mol%) phosphors, and (*c*) CIE 1931 coordinates of $LaCePO_4$:Dy^{3+} (2.5 mol%) phosphors ($x = 0.26$ and $y = 0.30$).

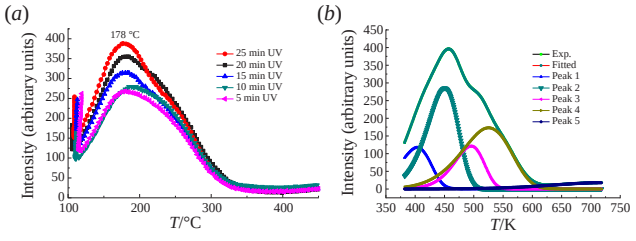

Figure 4 (*a*) TL glow curves of $LaCePO_4$:Dy^{3+} (2.5 mol%) phosphor at various UV exposure times; (*b*) CGCD pattern of TL glow curve of $LaCePO_4$:Dy^{3+} (2.5 mol%) phosphor after 25 min UV exposure.

parameters and frequency factors are given in Table 1. Here, most of the peaks show the first and general order of kinetics, and the values of shape factor μ from 0.37 to 0.46 indicate the position of trapped electrons in the luminescence center. The one electron trapped in the trap center for each peak for the UV irradiated phosphor shows the shallower trapping phenomenon. The CGCD pattern[27,28] of the prepared phosphor for 25 min UV exposure is shown in Figure 4(*b*).

In summary, dysprosium-doped lanthanum cerium phosphate phosphor showed good PL spectra in the blue and yellow regions which may be applicable for white light emission in various electronic devices. The crystal structure and morphology indicated the practical usability of the prepared phosphors. The PL emission spectra contain peaks at 475 and 573 nm, and the corresponding CIE coordinates $x = 0.26$ and $y = 0.30$ are very close to white light. The TL glow curve showed a broad intense

Table 1 Various trap parameters calculated using CGCD technique of the prepared $LaCePO_4$:Dy^{3+} (2.5 mol%) phosphor.[a]

Peak	T_1/K	T_m/K	T_2/K	τ/s	δ/K	ω/K	$\mu = \delta/\omega$	Activation energy E/eV	Frequency factor s/s^{-1}
1	371	403	431	32	28	60	0.46	1.84	7×10^{14}
2	414	449	471	35	22	57	0.38	1.9	2×10^{14}
3	457	497	521	40	24	64	0.37	1.88	2×10^{13}
4	472	525	567	53	42	95	0.44	1.53	4×10^{10}
5	587	669	720	82	51	133	0.38	1.35	2×10^{14}

[a] T_1 and T_2 are the low and high temperatures at the half maximum of the peak; T_m is the temperature at the peak maximum; τ is the mean lifetime; $\delta = T_2 - T_m$; $\omega = T_2 - T_1$.

peak centered at 178 °C, and the TL glow curve intensity increased with UV exposure time. The corresponding trap parameters were calculated using the CGCD technique. The trap depth varied from 1.35 to 1.9 eV, and the frequency factor was quite low varying from 4×10^{10} to 7×10^{14} s^{-1}. Therefore, the prepared phosphate-based phosphor may be useful for TL dosimetry applications.

Online Supplementary Materials

Supplementary data associated with this article can be found in the online version at doi: 10.1016/j.mencom.2024.06.041.

References

1 Z. C. Wu, J. X. Shi, J. Wang, M. L. Gong and Q. Su, *J. Solid State Chem.*, 2006, **179**, 2356.
2 M. Dyble, N. Narendran, A. Bierman and T. Klein, *Proc. SPIE*, 2005, **5941**, 291.
3 N. Narendran, L. Deng, R. M. Pysar, Y. Gu and H. Yu, *Proc. SPIE*, 2004, **5187**, 267.
4 E. F. Schubert and J. K. Kim, *Science*, 2005, **308**, 1274.
5 H. A. Höppe, *Angew. Chem., Int. Ed.*, 2009, **48**, 3572.
6 Y. Murayama, *Nikkei Science*, 1996, **26**, 20.
7 L. Jiang, C. Chang and D. Mao, *J. Alloys Compd.*, 2003, **360**, 193.
8 N. Kodama, T. Takahashi, M. Yamaga, Y. Tanii, J. Qiu and K. Hirao, *Appl. Phys. Lett.*, 1999, **75**, 1715.
9 N. Kodama, Y. Tanii and M. Yamaga, *J. Lumin.*, 2000, **87**–**89**, 1076.
10 S. Abe, K. Uematsu, K. Toda and M. Sato, *J. Alloys Compd.*, 2006, **408**–**412**, 911.
11 J. Kuang, Y. Liu and B. Lei, *J. Lumin.*, 2006, **118**, 33.
12 Y. Lin, Z. Tang, Z. Zhang and C. W. Nan, *J. Alloys Compd.*, 2003, **348**, 76.
13 L. Jiang, C. Chang, D. Mao and B. Zhang, *Mater. Lett.*, 2004, **58**, 1825.
14 Y. Wang, Z. Wang, P. Zhang, Z. Hong, X. Fan and G. Qian, *Mater. Lett.*, 2004, **58**, 3308.
15 J. Lü, Y. Huang, Y. Tao and H. J. Seo, *J. Alloys Compd.*, 2010, **500**, 134.
16 H. L. Ngee, T. Hatsumori, K. Uematsu, T. Ishigaki, K. Toda and M. Sato, *Phys. Procedia*, 2009, **2**, 171.
17 X. Hu, S. Yan, L. Ma, G. Wan and J. Hu, *Powder Technol.*, 2009, **192**, 27.
18 N. O. Nuñez, S. R. Liviano and M. Ocaña, *J. Colloid Interface Sci.*, 2010, **349**, 484.
19 R. Hussin, S. Hamdan, D. N. F. A. Halim and M. S. Husin, *Mater. Chem. Phys.*, 2010, **121**, 37.
20 P. Muralimanohar, G. Srilatha, K. Sathyamoorthy, P. Vinothkumar, M. Mohapatra and P. Murugasen, *Optik*, 2021, **225**, 165807.
21 K. A. Denault, J. Brgoch, M. W. Gaultois, A. Mikhailovsky, R. Petry, H. Winkler, S. P. DenBaars and R. Seshadri, *Chem. Mater.*, 2014, **26**, 2275.
22 P. F. Smet, A. B. Parmentier and D. Poelman, *J. Electrochem. Soc.*, 2011, **158**, R37.
23 R. Koutavarapu, M. R. Tamtam, S.-G. Lee, M. C. Rao, D.-Y. Lee and J. Shim, *J. Environ. Chem. Eng.*, 2021, **9**, 105893.
24 K. Ravindranadh, B. Babu, M. C. Rao, J. Shim, Ch. V. Reddy and R. V. S. S. N. Ravikumar, *J. Mater. Sci.: Mater. Electron.*, 2015, **26**, 6667.
25 V. Dubey, J. Kaur, N.S. Suryanarayana and K. V. R. Murthy, *Res. Chem. Intermed.*, 2014, **40**, 531.
26 J. W. Kaiser and W. Jeitschko, *Z. Kristallogr. – New Cryst. Struct.*, 2002, **217**, 25.
27 K. S. Chung, H. S. Choe, J. I. Lee, J. L. Kim and S. Y. Chang, *Radiat. Prot. Dosim.*, 2005, **115**, 343.
28 S. Som, M. Chowdhury and S. K. Sharma, *Radiat. Phys. Chem.*, 2015, **110**, 51.

Received: 4th March 2024; Com. 24/7410